

# Simple Semi-Analytical Septum Design for Improved Matching in Open TEM Cells

Giacomo Giannetti, *Graduate Student Member, IEEE*, Christian Spindelberger, *Student Member, IEEE*, and Holger Arthaber, *Senior Member, IEEE*

**Abstract**—Open transverse electromagnetic (TEM) cells are used for many applications. Usually, such cells are built of metal sheets with linear profiles. Due to these simple geometries, the impedance matching is limited. To improve the matching, a simple semi-analytical method for an advanced septum profile is developed. Dominant TEM-mode propagation and an expression for the characteristic impedance of a stripline are considered. The characteristic impedances of the feed and the central stripline are equal to a given, desired value. To minimize reflections, the characteristic impedance of the TEM mode is enforced to be constant over the entire structure, especially along the tapered sections. In this way the proposed method returns the septum width as a function of the longitudinal coordinate along the cell such that each cross-section has a characteristic impedance equal to the given, desired value. A septum designed according to the proposed method is manufactured and installed in a TEM cell prototype. The 30 MHz – 1 GHz frequency range is considered to cover CISPR bands C and D. Both measurements and full-wave simulations indicate an improvement in the return loss of 4.6 dB from 10.6 dB to 15.2 dB with respect to the previously installed linearly tapered septum.

**Index Terms**—Design methodology, Electromagnetic compatibility and interference, Impedance matching, Mathematical models, Stripline, TEM cells

## I. INTRODUCTION

Transverse electromagnetic (TEM) cells are devices used to generate highly uniform field patterns. As TEM cells are easy to build and low-cost, they are used in a wide variety of applications. For instance, they are successfully used for dielectric characterizations [1], [2] in [3], for biological cell exposure in [4], and for EMC/EMI pre-compliance tests in [5], [6].

The key parameters describing the performance of TEM cells are the impedance matching, the bandwidth, the field homogeneity, and the usable test-volume. These parameters are strongly coupled. Indeed, the bandwidth and the field homogeneity decrease for a larger test-volume due to the excitation of higher order modes [7] and a better impedance matching implies a better field homogeneity [8]. The impedance matching is quantified in terms of return loss (RL).

G. Giannetti is with the Department of Information Engineering, University of Florence, 50121 Florence, Italy (e-mail: giacomo.giannetti@unifi.it).

C. Spindelberger and H. Arthaber are with the Department of Electrodynamics Microwave and Circuit Engineering, Technical University of Vienna, 1040 Vienna, Austria.

Manuscript received -; revised -. (Corresponding author: G. Giannetti).

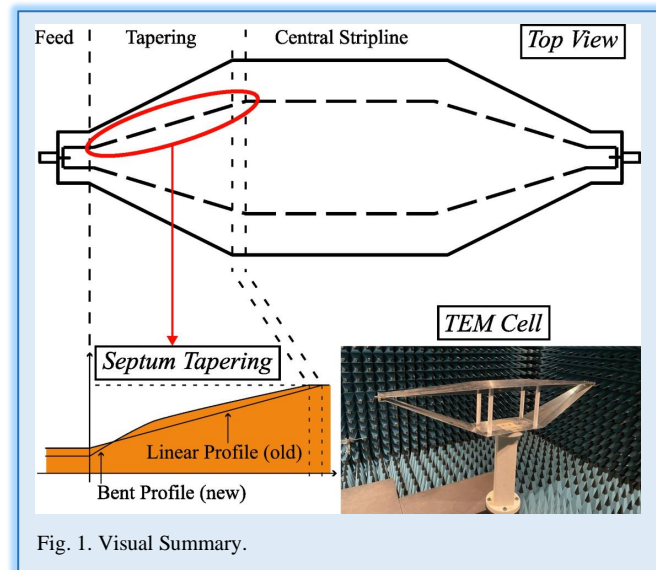


Fig. 1. Visual Summary.

TEM cells' RL should be at least 10 dB [9]. However, there is a great interest in further improving matching due to certain EMC standard requirements. For instance, [10] indicates that a RL of at least 14 dB is desirable. Besides, a better impedance matching leads to less absolute measurement uncertainties due to load mismatches [11].

In TEM cells, a very critical part for the degradation of RL is the tapering [10], [12], which connects the feed with the central stripline. Several works operate on the tapering to improve the RL. In [10], the original linear straight tapering from [13] is studied extensively with a special focus on its start and end points. On the other hand, in [12], different arguments based on the characteristic impedance along the septum are analyzed to improve matching by means of both multi-step and piecewise linear tapering. Both [10] and [12] rely on optimizations performed over computationally expensive full wave

### Take-Home Messages:

- Interest in improving TEM cell's impedance matching to improve field homogeneity and to reduce absolute measurement uncertainties
- Development of a new and simple semi-analytical design method for the septum's profile design
- Saving computational resources by avoiding expensive full-wave simulations and optimizations
- Validation of the method by improving an already existing TEM cell design
- Simulation and measurement results indicate a return loss increase of 4.6 dB from 10.6 dB to 15.2 dB with respect to the linearly tapered septum in the 30MHz – 1 GHz frequency range (CISPR bands C and D)

simulations and are time consuming, therefore.

Regarding the rigorous semi-analytical modeling of the TEM cell, mode matching [14] is applied in [15] to analyze closed TEM cells. However, open TEM cells, as those considered in our work, have openings which partially radiate. To consider this, a more sophisticated mode matching analysis, taking a continuous mode spectrum into account, would be required.

In our work, we focus on reflection reduction in open TEM cells by continuously modifying the septum geometry. This task is solved by means of a simple yet accurate semi-analytical method. We tackle the inherent difficulties of radiative and higher order modes by assuming that the TEM-mode propagation is dominant over the higher order modes. Particularly, based on an analytical expression for the characteristic impedance of the TEM cell's cross-section, a near-optimum profile for impedance matching within the tapering section is derived. The method requires no optimization and, therefore, the number of full-wave simulations is reduced. The proposed method is firstly derived for a generic case in Sec.II and secondly applied to the specific open TEM cell from [16] in Sec.III. Eventually, conclusions are drawn in Sec.IV and present work is summarized graphically in Fig. 1.

## II. SEPTUM DESIGN

TEM cells are composed of three parts: the feed, the tapering and the central stripline, as depicted in Fig. 1. All parts are striplines. However, the feed and the central stripline have constant transverse dimensions along the direction of propagation while the tapering has varying transverse dimensions to connect the narrow feed to the wide central stripline. In particular, the outer conductors are parallel to the septum for the feed and central stripline parts while this does not apply for the tapering sections. The three parts are connected such that the septum remains flat along the entire TEM cell and the outer conductors are bent to connect the feeds and the central stripline. For further details about the design of the TEM cell please refer to [16].

Exploiting transmission line theory and if TEM-mode is dominant over the higher order modes, the problem, neglecting the higher order modes, is visualized from an electrical perspective in Fig. 2. The feed and the central stripline have a  $z$ -independent characteristic impedance equal to  $Z_f$  and  $Z_s$ , respectively. On the other hand, the tapering has a  $z$ -dependent characteristic impedance  $Z_c(z)$  and ranges from  $z = 0$  to  $z = l_2$ . The problem of joining two different waveguides with minimum reflections is well known [17]. Particularly, if the characteristic impedances of the two waveguides are equal, that is,  $Z_f = Z_s$ , then the optimum matching section is the one with a constant characteristic impedance equal to those of the two waveguides. If  $Z_f = Z_s = Z_d$ , where  $Z_d$  is a desired value, then the characteristic impedance along the tapering that minimizes the reflections is equal to  $Z_c = Z_d$  for each longitudinal coordinate  $z$  between 0 and  $l_2$ .

A generic stripline cross-section is depicted in Fig. 3. The outer conductors are grounded. Parameters describing the stripline cross-section are the distance between upper conductor and septum  $h_t$ , the septum height  $h_s$ , the width of the outer conductors  $w_c$ , the width of the septum  $w_s$ , and the thickness of the septum and outer conductors  $t_s$ . The background material has  $\epsilon_r = 1$  and  $\mu_r = 1$ . Generally speaking, the characteristic impedance for the TEM mode of the stripline depends on all the geometrical parameters of the stripline

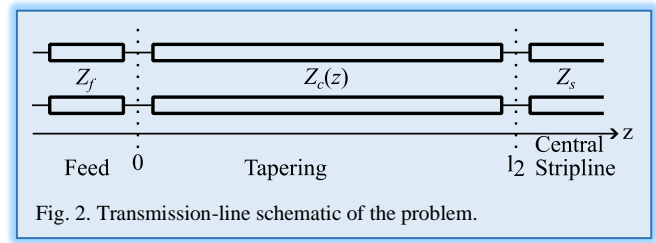


Fig. 2. Transmission-line schematic of the problem.

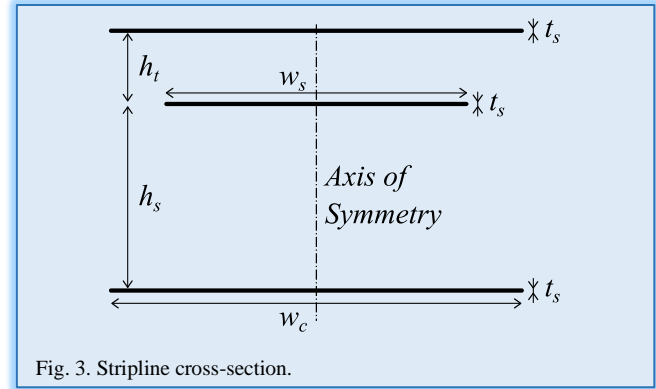


Fig. 3. Stripline cross-section.

cross-section and writes

$$Z_c = Z_c(h_t, h_s, w_c, w_s, t_s). \quad (1)$$

In the tapering, the quantities  $h_t$ ,  $h_s$ ,  $w_c$  and  $w_s$  depend on the longitudinal coordinate  $z$ , while the thickness  $t_s$  is constant.

There are three ways to achieve a constant characteristic impedance equal to  $Z_d$  along the tapering of the cell. They are a) bend one or both outer conductors and keep a linear straight septum profile, b) keep linear straight outer conductors and modify the septum profile, and c) modify the other conductors' width. In case a) we would vary  $h_t$  or  $h_s$ , in case b)  $w_s$ , and in case c)  $w_c$ . All solutions are equivalent from an electrical point of view. However, approach b) is the easiest to implement in practice and hence pursued in our work.

A pictorial representation of the problem is drawn in Fig. 4. In the upper graph of Fig. 4, the lateral view of the TEM cell is shown. The longitudinal coordinate  $z = 0$  mm is aligned with the end of the feed and the beginning of the tapering. The end of the bends of the outer conductors is at  $z = l_1$  while the tapering of the septum is in  $0 \text{ mm} \leq z \leq l_2 \neq l_1$ . This is the same as in the original approach by Crawford [13]. However, in the proposed approach the tapering ends and the septum reaches the maximum width at  $z = l_1$ , since constant distances between outer conductors and septum for  $z \geq l_1$  imply a constant width for the septum itself in the range  $l_1 \leq z \leq l_2$ . The lower graph in Fig. 4 depicts the top view of the septum.

The boundary conditions of the problem are the following:  $h_t$  and  $h_s$  at  $z = 0$  mm and at  $z = l_1$  are given; the stripline width of the central stripline  $w_s(z = l_1)$  is also given and is such that it realizes the desired characteristic impedance in the central stripline; the end coordinate of the tapering  $l_1$  is provided. Expressions for the quantities  $h_t(z)$ ,  $h_s(z)$ , and  $w_c(z)$  are also given. Eventually, enforcing the condition  $Z_c(z) = Z_d$  along the tapering, an explicit equation with a unique solution defining an implicit function for  $w_s(z)$  is found. Particularly, for a given longitudinal coordinate  $\bar{z}$ , (1) becomes

$$Z_c(h_t(\bar{z}), h_s(\bar{z}), w_c(\bar{z}), w_s(\bar{z}), t_s) = Z_d \quad (2)$$

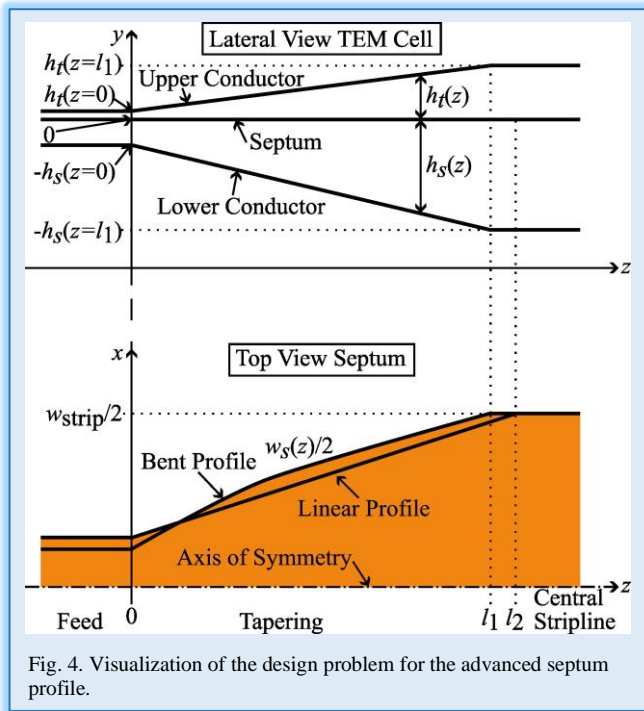


Fig. 4. Visualization of the design problem for the advanced septum profile.

and can be solved for  $w_s(\bar{z})$ . Assuming that the tapering is gradual and that it is long enough for the stabilization of the field mode, the solution to (2) for all  $z$  between 0 mm and  $l_1$  returns a near-optimal septum profile for RL maximization.

### III. RESULTS

The proposed method is now applied to the TEM cell described in [16]. For this case we have  $l_1 = 621.9$  mm,  $t_s = 3$  mm,  $h_t(z = 0 \text{ mm}) = 7$  mm,  $h_t(z = l_1) = 41.4$  mm,  $h_s(z = 0 \text{ mm}) = 10$  mm, and  $h_s(z = l_1) = 300$  mm. For the new septum it is  $l_2 = l_1$  while it is  $l_2 = 641.9$  mm for the one presented in [16]. The width of the septum in the central stripline realizing the desired characteristic impedance is  $w_s(z = l_1) = 195$  mm. The  $y$ -distance between upper conductor and septum  $h_t(z)$  and the one between lower conductor and septum  $h_s(z)$  (see Fig. 4) vary linearly in the interval  $0 \text{ mm} \leq z \leq l_1$  according to

$$h_t(z) = h_t(z = 0 \text{ mm}) + \frac{z}{l_1}(h_t(z = l_1) - h_t(z = 0 \text{ mm})) \quad (3a)$$

$$h_s(z) = h_s(z = 0 \text{ mm}) + \frac{z}{l_1}(h_s(z = l_1) - h_s(z = 0 \text{ mm})). \quad (3b)$$

Among all the formulae for the computation of the characteristic impedance (1), e.g., [18], [19], the one in [20] is considered in the following since it represents a good compromise between accuracy and implementation complexity. The characteristic impedance for the TEM mode of the stripline writes (from (2) in [20]):

$$Z_c = Z_0 \left( \frac{(w/b)_{eff}}{\gamma} + \frac{(w/b)_{eff}}{\beta - \gamma} + \frac{2c'_f}{\epsilon_0} \right)^{-1} \quad (4)$$

where  $\epsilon_0$  is the vacuum permittivity and  $(w/b)_{eff}$ ,  $\gamma$ ,  $\beta$ , and  $c'_f$  are quantities depending on the geometrical parameters  $h_s$ ,  $h_t$ ,  $w_s$ , and  $t$  as defined in [20]. In (4), an infinite width for the outer conductors of the stripline ( $w_c = \infty$ ) is considered while in practice a stripline has a finite width. Due to this, there is a slight deviation from the impedance characteristic foreseen by (4) and the actual, i.e., from simulations, characteristic impedance. To compensate this a desired characteristic impedance equal to  $Z_d = 49 \Omega$  is enforced. In this way an actual characteristic impedance of  $50 \Omega$  is achieved.

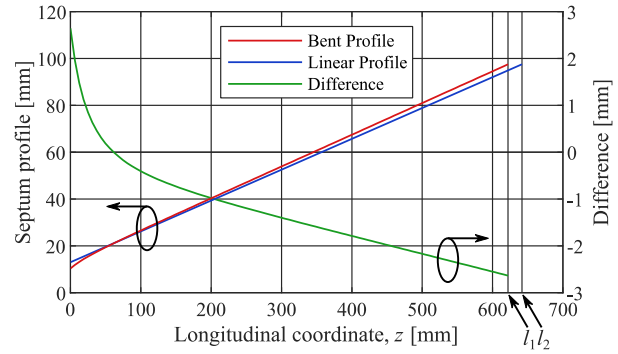


Fig. 5. Bent and linear profiles, and difference between them. The coordinates refer to the septum top view of Fig. 4. The circles and the arrows upon them indicate the vertical scale to which the curves refer.

Unfortunately, despite its simplicity, (4) contains elliptic integrals and hyperbolic functions (see [20] for details) and then (2) cannot be worked out to get  $w_c(z)$  explicitly. Although an analytic solution in power series could be sought for, the problem (2) is more easily solved numerically with a zero-finding algorithm. Particularly, problem (2) is solved over 101 evenly spaced points in the interval  $0 \text{ mm} \leq z \leq l_1$ . The  $z$ -distance between successive points is then  $l_1/100 = 6.219$  mm. These points are joined with straight lines, creating the profile shown in Fig. 5. In the same figure also the old linear design for  $w_s(z)$  and the difference between old and new profiles are depicted. Note that the maximum difference between the profiles is less than 3 mm and that the new profile tends to become linear increasing the longitudinal coordinate. The derivative of the new profile  $w_s(z)$  with respect to the longitudinal coordinate is greater closer to the feed and tends to become constant far away from it. The widths of new and old profiles are 20.7 mm and 26.0 mm at  $z = 0$  mm, respectively.

The derived septum profile is fabricated of aluminum using a laser cutting machine achieving manufacturing tolerances in the 0.1 mm range. The new septum mounted on the TEM cell around a feed is depicted in Fig. 6 while the entire TEM cell with the new septum is shown in Fig. 1.

The TEM cell is simulated in ANSYS HFSS [21] in the frequency interval 30 MHz – 1 GHz considering the FEM solver and the broadband adaptive mesh. This frequency range is chosen to cover CISPR bands C and D. The TEM cell is measured in an anechoic chamber to avoid any influence of the surroundings.

Measured and simulated magnitudes of the  $S_{11}$  scattering parameter are depicted in Fig. 7. Measured data for the linearly tapered septum in [16] are also drawn. We notice an overall good agreement between simulations and measurements. Resonance frequencies from both measurements and simulations coincide well even if minima in the magnitude of the reflection coefficient from measurements are generally less sharp. Furthermore, the deviations in the  $|S_{11}|$ , especially those for frequencies below 300 MHz, result from constructional and mounting imperfections and a limited VNA accuracy for small magnitude values. The minimum value for the measured RL in the frequency range 30 MHz – 1 GHz is 15.2 dB at 825 MHz. This value is 4.6 dB greater than the minimum value of RL for the TEM cell in [16] in the same bandwidth, thus proving the effectiveness of the proposed design method.



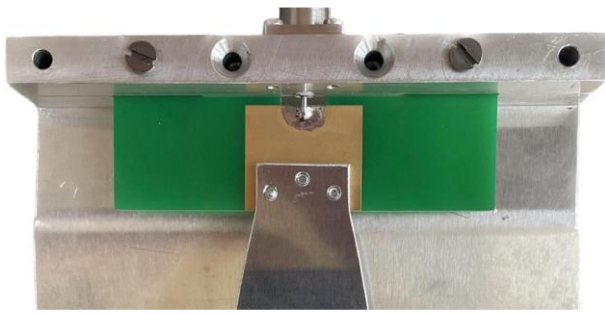


Fig. 6. An extremity of the new septum mounted on the TEM cell.

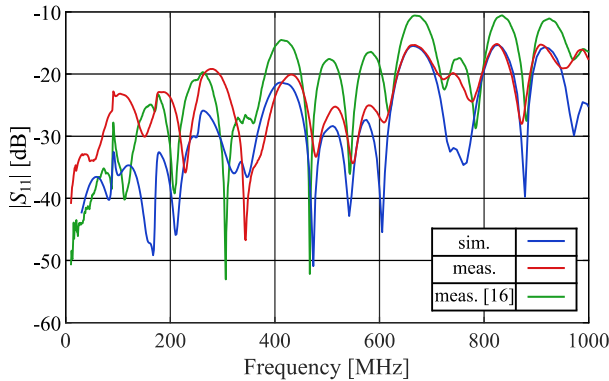


Fig. 7. Simulated and measured magnitudes of the scattering parameters.

#### IV. CONCLUSIONS

A simple semi-analytical design method based on dominant TEM-mode propagation for RL improvement in open TEM cell is presented. This method realizes a constant characteristic impedance along the tapering of the TEM cell, equal to the value of the characteristic impedance of both the feeds and the central stripline. The profile of the septum manufactured following the proposed approach differs less than 3 mm from the linear profile previously mounted on the same TEM cell. However, it improves remarkably the RL of 4.6 dB from 10.6 dB to 15.2 dB compared to the linearly tapered septum. The new minimum value of the RL is greater than the target value of 14 dB. Additionally, the present method saves computational resources since it does not rely on optimizations.

As future developments, it would be interesting to perform a time domain reflectometry analysis aimed at investigating the locations at which reflections occur and to develop advanced modelling techniques that help improving the TEM cell RL further.

#### V. CONFLICT OF INTEREST

The authors have no conflict of interest to disclose.

#### REFERENCES

- [1] M. Mertens, M. Chavoshi, O. Peytral-Rieu, K. Grenier, and D. Schreurs, "Dielectric spectroscopy: Revealing the true colors of biological matter," *IEEE Microw. Mag.*, vol. 24, no. 4, pp. 49–62, 2023.
- [2] G. Giannetti and K. Klinkenbusch, "Interpretation and separability of the effective permittivity in case that both permittivity and conductivity are complex," in *Proc. Electromagn. Theory Symp.*, 2023.
- [3] S. Yee, A. Sayegh, A. Kazempour, and M. M. Jenu, "Design and calibration of a wideband TEM-cell for material characterization," in *2012 Asia-Pacific Symp. Electromagn. Compat.* IEEE, 2012, pp. 749–752.
- [4] M. Soueid, S. Kohler, L. Carr, S. M. Bardet, R. P. O'Connor, P. Leveque, and D. Arnaud-Cormos, "Electromagnetic analysis of an aperture modified TEM cell including an ITO layer for real-time observation of biological cells exposed to microwaves," *Prog. Electromagn. Res.*, vol. 149, pp. 193–204, 2014.

- [5] R. Videnka and J. Svacina, "Introduction to EMC pre-compliance testing," in *2008-17th Int. Conf. Microw. Radar Wireless Commun.* IEEE, 2008, pp. 1–4.
- [6] S. M. Satav and V. Agarwal, "Do-it-Yourself Fabrication of an Open TEM Cell for EMC Pre-compliance," *IEEE EMC Soc. Newsl.*, no. 20, 2008.
- [7] P. F. Wilson and M. T. Ma, "Simple approximate expressions for higher order mode cutoff and resonant frequencies in TEM cells," *IEEE Trans. Electromagn. Compat.*, vol. 28, no. 3, pp. 125–130, 1986.
- [8] S. Deng, D. Pommerenke, T. Hubing, and D. Shin, "An experimental investigation of higher order mode suppression in TEM cells," *IEEE Trans. Electromagn. Compat.*, vol. 50, no. 2, pp. 416–419, 2008.
- [9] *CISPR 16-1-1 Specification for radio disturbance and immunity measuring apparatus and methods - Part 1-1: Radio disturbance and immunity measuring apparatus - Measuring apparatus*, International Electrotechnical Commission (IEC) Std. CISPR 16-1-1:2019.
- [10] P. Alotto, D. Desideri, and A. Maschio, "Parametric analysis and optimization of the shape of the transitions of a two-port rectangular TEM cell," in *IEEE Int. Symp. Electromagn. Compat.*, 2012.
- [11] K. Patel and P. Negi, "Importance and estimation of mismatch uncertainty for RF parameters in calibration laboratories," *Int. J. Metrol. Qual. Eng.*, vol. 3, no. 1, pp. 29–37, 2012.
- [12] M. Arezoomand, M. Kalantari Meybodi, and N. Noori, "Design of a TEM cell using both multi-step and piecewise linear tapering," in *2016 8th Int. Symp. Telecommun.*, 2016, pp. 571–574.
- [13] M. L. Crawford, "Generation of standard EM fields using TEM transmission cells," *IEEE Trans. Electromagn. Compat.*, no. 4, pp. 189–195, 1974.
- [14] G. G. Gentili, G. Giannetti, G. Pelosi, and S. Selleri, "Transformation optics combined with line-integrals for fast and efficient mode matching analysis of waveguide devices," *IEEE J. Microw.*, pp. 1–10, 2023.
- [15] U. Balaji and R. Vahldieck, "Analysis of higher order modes in TEM cells and RCL using the mode matching method," in *1995 Int. Conf. Electromagn. Interference Compat.*, 1995, pp. 259–262.
- [16] C. Spindelberger, G. Giannetti, and H. Arthaber, "Increasing the Test-Volume of Open TEM Cells by Using an Asymmetric Design," in *2022 Kleinheubach Conf. IEEE*, 2022, pp. 1–4.
- [17] R. P. Hecken, "A near-optimum matching section without discontinuities," *IEEE Trans. Microw. Theory Tech.*, vol. 20, no. 11, pp. 734–739, 1972.
- [18] E. Costamagna and A. Fanni, "Asymmetric TEM cell impedance calculation," in *IEE Proc. H-Microw. Antennas Propag.*, vol. 137, no. 5, IET, 1990, pp. 318–320.
- [19] M. Lucido, G. Panariello, and F. Schettino, "Accurate and efficient analysis of stripline structures," *Microw. Opt. Technol. Lett.*, vol. 43, no. 1, 2004.
- [20] P. Robrish, "An analytic algorithm for unbalanced stripline impedance," *IEEE Trans. Microw. Theory Tech.*, vol. 38, no. 8, 1990.
- [21] ANSYS. (2022) Ansys — engineering simulation software. [Online]. Available: <https://www.ansys.com/>